Temperature-dependent phase transition in barium titanate crystals probed by second harmonic generation

Jiesu Wang, Kuijuan Jin, Hongbao Yao, Junxing Gu, Xiulai Xu, Chen Ge, Can Wang, Meng He, and Guozhen Yang

Citation: Appl. Phys. Lett. **112**, 102904 (2018); doi: 10.1063/1.5023293
View online: https://doi.org/10.1063/1.5023293
View Table of Contents: http://aip.scitation.org/toc/apl/112/10
Published by the American Institute of Physics

Temperature-dependent phase transition in barium titanate crystals probed by second harmonic generation

Jiesu Wang,[1,2] Kuijuan Jin,[1,2,3,a)] Hongbao Yao,[1,2] Junxing Gu,[1,2] Xiulai Xu,[1,2] Chen Ge,[1] Can Wang,[1] Meng He,[1] and Guozhen Yang[1,3]

[1]*Beijing National Laboratory for Condensed Matter Physics, Institute of Physics, Chinese Academy of Sciences, Beijing 100190, China*
[2]*School of Physical Sciences, University of Chinese Academy of Sciences, Beijing 100190, China*
[3]*Collaborative Innovation Center of Quantum Matter, Beijing 100190, China*

(Received 23 January 2018; accepted 17 February 2018; published online 8 March 2018)

More and more evidence points out the coexistence of displacive and order-disorder dynamics in the phase transition of barium titanate. Here, we report an initial state determined phase transition in barium titanate by applying second harmonic generation technology and piezoresponse force microscopy (PFM). The out-of-plane PFM results of these barium titanate crystals show the increase in domain walls in the surfaces after annealing, leading to the increase in the second harmonic signal measured. This work directly revealed how the displacive and order-disorder dominate the phase transition and what the role is that the domain wall plays in this process. *Published by AIP Publishing.* https://doi.org/10.1063/1.5023293

Over the past several years, the dynamics of ferroelectric phase transition in ferroelectric materials was classified in terms of being either displacive or order-disorder type.[1] Nowadays, more and more theoretical calculations and experimental data have proved that the two types of dynamics coexist in the ferroelectric phase transition of barium titanate.[2,3] Barium titanate ($BaTiO_3$, BTO) is a typical perovskite oxide ferroelectric, which belongs to one of the most interesting material classes because of its huge potential applications as well as its broad range of understanding the basic physics.[4,5] BTO undergoes three structural phase transitions with the temperature decrease—at around 125 °C from cubic to tetragonal, along with the paraelectric phase to the ferroelectric phase; at around 0 °C from tetragonal to orthorhombic; and at around −90 °C from orthorhombic to rhombohedral.[6]

For the phase transition of BTO around its ferroelectric curie temperature $T_C = 125$ °C, second-harmonic generation (SHG) should be a perfect technique to indicate this process[7–9] because SHG is only allowed in noncentrosymmetric structures in the leading electric-dipole (ED) order.[10] Therefore, the finding of a finite integral SHG signal in the cubic paraelectric phase of BTO was thought of as a most surprising experimental result. The explanation of the occurrence of the unexpected SHG signal includes local broken symmetry caused by defects, pinning effects by polar molecules, quantum paraelectric, and ferroelectric fluctuation.[11,12] In this paper, we use the typical reflected SHG technique to prove the coexistence of displacive and order-disorder dynamics in the phase transition of barium titanate and demonstrate that the initial state of the ferroelectric material will determine the kinetic mechanism of phase transformation around T_C. Using piezoresponse force microscopy (PFM) and atomic force microscopy (AFM), we also illustrate the role that domain walls play in the phase transition of barium titanate.

We use two types of BTO single crystals grown by the top seeded solution growth (TSSG) method. One type is the (001)-oriented BTO single crystal with the polarization coherently polarized along the surface normal and the other is the (100)-oriented BTO single crystal with random polarization orientation near the surface. The typical reflected SHG configuration employed is shown in Fig. 1. The incident laser is generated from a mode-lock femtosecond (fs) Ti:Sapphire oscillator (Tsunami 3941-X1BB, Spectra Physics) with a central wavelength at 800 nm, a pulse duration of about 100 fs, a repetition rate of 82 MHz, and the energy rate attenuated to 70 mW before being focused. Based on the different polarization combinations of the incident and reflected light, two configurations were employed. One is denoted by *p-out*, for the analyzer polarization parallel to the plane of incidence and the incident light polarization being rotated, and the other is denoted by *s-out*, for the analyzer polarization perpendicular to the plane of incidence and the incident light polarization being rotated.

The relationship between the intensity of SHG from a non-centrosymmetry crystal and its nonlinear polarization is $I_{(2\omega)} \propto |P_{(2\omega)}|^2$. The SH light intensity is also directly

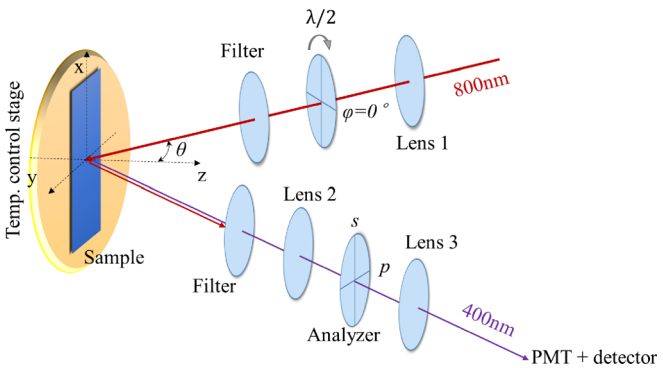

FIG. 1. Typical reflected SHG configuration. θ is the angle between incident light and the sample normal, set as 45°. φ stands for the polarization of incident fundamental light, which is controlled by a half-wave ($\lambda/2$) plate assembled on a stepping motor manipulated by computer. Lens 1 and lens 3 are for focusing the laser, while lens 2 is for collimating. The coordinate system is established as shown which is not sample dependent.

a)Author to whom correspondence should be addressed: kjjin@iphy.ac.cn

proportional to the sum of SH photons $S_{(2\omega)}$, under the coordinate shown in Fig. 1, which can be written as $S_{(2\omega)} \propto |\vec{e}''_{2\omega} \cdot \overleftrightarrow{\chi}^{(2)} : \vec{e}''_{\omega}\vec{e}''_{\omega}|^2$.[10] The surface symmetries of the polarized (001) BTO and the non-polarized (100) BTO crystals belong to the point groups of *4 mm* and *m*, respectively. The optical second-order susceptibility tensors of symmetry *4 mm* and symmetry *m* (the mirror plane is aligned parallel to the incident plane) are in the forms of

$$\overleftrightarrow{\chi}^{(2)}_{4\,mm} = \begin{pmatrix} 0 & 0 & 0 & 0 & \chi_{15} & 0 \\ 0 & 0 & 0 & \chi_{15} & 0 & 0 \\ \chi_{31} & \chi_{31} & \chi_{33} & 0 & 0 & 0 \end{pmatrix} \tag{1}$$

and

$$\overleftrightarrow{\chi}^{(2)}_{m} = \begin{pmatrix} \chi_{11} & \chi_{12} & \chi_{13} & 0 & \chi_{15} & 0 \\ 0 & 0 & 0 & \chi_{24} & 0 & \chi_{26} \\ \chi_{31} & \chi_{32} & \chi_{33} & 0 & \chi_{35} & 0 \end{pmatrix}, \tag{2}$$

respectively.[14] Substituting Eqs. (1) and (2) into the expression of $S_{(2\omega)}$, we can derive the specific expressions of $S_{(2\omega)}$ in *4 mm* and *m* symmetries, respectively, under the two configurations *p-out* and *s-out*, namely,

$$\begin{cases} S_{4\,mm,p-out} \propto \left(\mathrm{A}\cos^2\varphi - B\sin^2\varphi\right)^2, \\ S_{4\,mm,s-out} \propto \left(\mathrm{C}\sin 2\varphi\right)^2, \end{cases} \tag{3}$$

$$\begin{cases} S_{\mathrm{m},p-out} \propto \left(D\sin 2\varphi + E\cos^2\varphi - F\sin^2\varphi\right)^2, \\ S_{m,s-out} \propto \left(H\sin 2\varphi + I\cos^2\varphi + J\sin^2\varphi\right)^2, \end{cases} \tag{4}$$

where L^{Ω}_{xx}, L^{Ω}_{yy}, and L^{Ω}_{zz} are the three nonvanishing diagonal elements of transmission Fresnel tensor at frequency Ω.[14] What the letters A∼J denote for can be found in our former research as Ref. 13. The theoretical expression groups (3) and (4) are used to fit the experimental results, illustrating the symmetry variation of the BTO crystal surfaces.

The samples are all heated from room temperature (RT) to 400 °C and then cooled back to RT. In this process, the SHG signals are measured at each fixed temperature point after being maintained for 30 s. The results of temperature dependence of the normalized SHG signal $I^{2\omega}_{Norm} = I^{2\omega}_{(T)}/I^{2\omega}_{(25\,^\circ\mathrm{C})}$ is presented in Fig. 2, for $\varphi = 0^\circ$ under the *p-out* configuration.

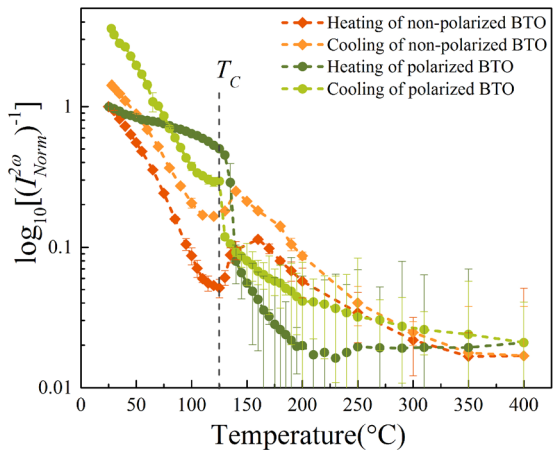

FIG. 2. The temperature dependence of the normalized SHG signal $I^{2\omega}_{Norm} = I^{2\omega}_{(T)}/I^{2\omega}_{(25\,^\circ\mathrm{C})}$ for the polarized and non-polarized BTO crystals. The gray dashed lines denote the Curie temperature T_C of BTO at 125 °C.

Here, $I^{2\omega}_{(T)}$ and $I^{2\omega}_{(25\,^\circ\mathrm{C})}$ are the SHG intensities at the current temperature and RT, respectively. It can be obviously seen that the SHG intensities decrease as the temperature increases, generally in both cases, while the SHG intensity of the non-polarized (100) BTO drops much faster than that of the polarized (001) BTO at the very beginning of the temperature-rising process. This difference might be the result of the off-center Ti displacement pinned by the charged ions deposited on the surface of the polarized samples.[11] This pinning effect might also cause the distinct difference in the heating and cooling slopes of the polarized (001) BTO, for there is no deposited surface ion engaged in the process cooling from its cubic phase.

When the samples are heated over the T_C (125 °C), the SHG intensity of the polarized (001) BTO falls rapidly, implying the process of phase transition from tetragonal to cubic. Meanwhile, the most interesting phenomenon appears that in the non-polarized (100) BTO, the SHG intensity recovers to a peak of 10% of initial SHG intensity at the temperature $T_C + \sim 30\,^\circ\mathrm{C}$ and then keeps the dropping tendency until a negligible low level. This behavior will also be discussed in detail later.

In the subsequent cooling process, a remarkable hysteresis in both types of BTO crystals was observed. Although the hysteresis curves show different loop shapes and reversing direction, a higher SHG intensity was observed in both cases compared with their initial SHG intensity correspondingly, while the increase for the polarized (001) BTO is larger than that for the non-polarized (100) BTO.

To explore the specific evolution of structure symmetry in the temperature changing process, we carried out the *in-situ* polarization-dependent SHG measurement in the selected temperatures when BTO exhibiting different phases, as shown in Fig. 3. For the polarized (001) BTO, the SHG patterns have kept their shapes during the heating process, in both its tetragonal phase [Fig. 3(a)] and cubic phase [Fig. 3(b)], with the *p-out* patterns characterized by a twofold rotational symmetry possessing two major peaks and two minor ones and the *s-out* patterns characterized by a fourfold rotational symmetry. This uniformity demonstrates that the structural symmetry of the surface of polarized (001) BTO has been maintained in the heating process, which belongs to the *4 mm* point group,[15] and no in-plane polarization occurred. For the cubic phase of non-polarized (100) BTO, the situation is similar to our former research on the cubic $SrTiO_3$ surface whose point group is also *4 mm*, and thus, the SHG patterns in Fig. 3(e) are consistent with those in Figs. 3(a) and 3(b). Theoretical simulations (solid lines) have a good agreement with the experimental data (discrete points) when substituting the expression (3) in Figs. 3(a), 3(b), and 3(e).

Figure 3(d) presents the *p-out* and *s-out* SHG patterns of non-polarized (100) BTO at RT, whose polarization direction is mainly in-plane.[4] The solid lines in Fig. 3(d) are the theoretical simulations under the assumption that the surface symmetry belongs to the *m* point group.

Figures 3(c) and 3(f) show the SHG polar plots of the two types of crystals cooled back to RT. A thermal annealing will destroy the ferroelectric ordering in BTO,[16] leading to a multi-domain structure in the crystals. We assume that the surface symmetry of the BTO crystals cooled back to RT is a

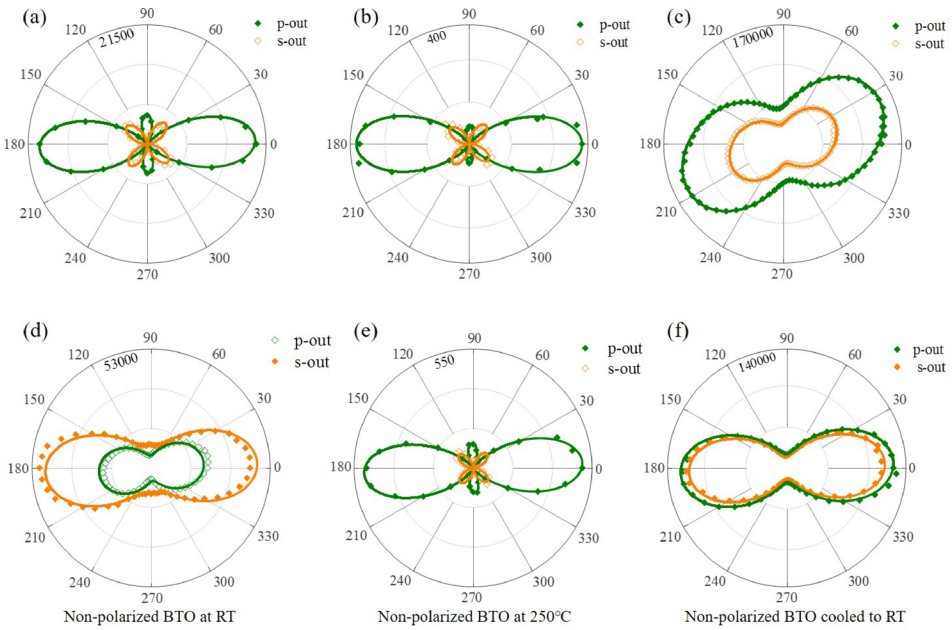

FIG. 3. *In-situ* polarization-dependent SHG polar plots for the polarized (001) BTO crystal at (a) RT, (b) 250 °C, and (c) cooled back to RT and the non-polarized (100) BTO crystal at (d) RT, (b) 250 °C, and (c) cooled back to RT. The solid and hollow points are experimental data, and the solid lines are theoretical fittings.

combination of *4 mm* where the polarization is out-of-plane and *m* where the polarization is in-plane. The solid lines in Figs. 3(c) and 3(f) are the theoretical simulation based on the above assumption, having a good fit with the experimental data.

The out-of-plane domain evolution on the surfaces of the two types of BTO crystals is demonstrated by PFM technology, as shown in Fig. 4. We marked an area of 30 μm $\times$ 30 μm on each type of BTO crystal. The PFM images make it clear that in both cases the amount of domains with random poling directions increased after the sample being annealed, which gave rise to an increase in domain walls at the surface as well as the SH signal generated from the surface. From Fig. 2, it can be found that the increasing degree of SHG intensity from unity to disorder of the surface of polarized (100) BTO is higher than that from disorder to more disorder of the surface of non-polarized (001) BTO.

The ferroelectric phase transition in BTO was once thought displacive,[17] until some experimental and theoretical evidence proved the coexistence of a displacive and order-disorder component in its phase transition mechanism.[2,3,18] Figure 5 visually exhibits the difference in displacive and order-disorder mechanisms. It is theoretically predicted that the SHG intensity in ferroelectrics is proportional to the spontaneous polarization,[11] and thus, the displacive phase transition from low-temperature to high-temperature would be accompanied by the decrease in the SHG intensity of ferroelectric materials. While the order-disorder mechanism would definitely cause the excess domains, and the emerging domain walls where net polarizations exist must contribute more SHG signals.

For the polarized (001) BTO before being heated, the SH signals are derived from the breaking of the center symmetry along the direction out-of-plane, including polarization-induced

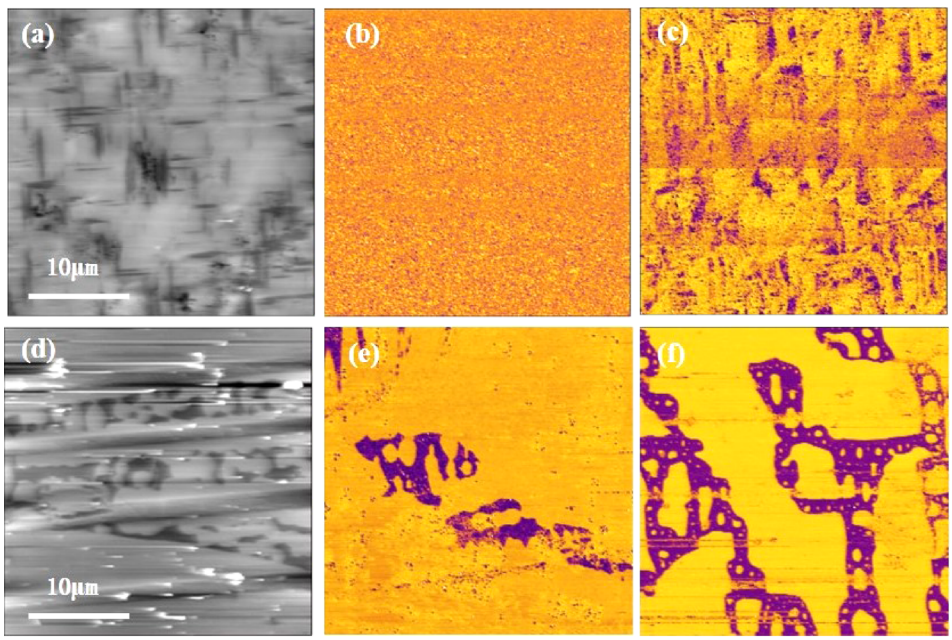

FIG. 4. (a) and (d) are the AFM results of areas on the surfaces of polarized (001) BTO and non-polarized (100) BTO crystals, respectively. (b) and (e) are the corresponding out-of-plane PFM phase image of (a) and (d) before the sample being heated. (c) and (f) are also the corresponding PFM phase image of (a) and (d), while after the sample being heated.

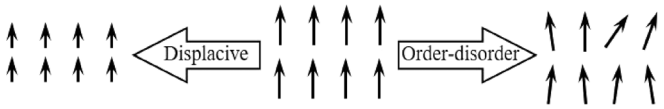

FIG. 5. Sketch of pure displacive and order-disorder ferroelectric phase transition mechanisms. The direction and length of the arrows indicate the direction and intensity of the ferroelectric polarization.

and surface-induced breaking. When the temperature exceeds T_C, the phase of the BTO crystal transforms from tetragonal to cubic, accompanied by the dramatic decrease in SHG intensity to more than 90% of the initial SHG intensity. A further decrease in the SH signal with the temperature can be explained by the heterogeneous media at the surface, local inhomogeneity, and the quantum paraelectric effect.[11,12,19–21] We speculate that in the polarized (001) BTO heating process, only displacive behavior appeared and the center symmetry breaking at the surface is always out-of-plane. This can explain why the shapes of the SHG patterns in Figs. 3(a) and 3(b) are the same, as well as other several temperature points between 25 °C and 200 °C in the heating process, which were not shown here.

As to the non-polarized (100) BTO, if there were only displacive behavior happened in the heating process, the SHG intensity around T_C should drop directly, the same as that for the polarized BTO. However, a distinct and unexpected recovery of the SHG intensity between T_C and $T_C + \sim 30$ °C is observed. This contradiction means that alongside the displacive transition, order-disorder transition also occurred, leading to the long-range order being destroyed and the domain walls showing up and thus the SHG intensity increasing. The competition between the two mechanisms leads to its special dropping tendency. The surficial symmetry of the cubic non-polarized (100) BTO at 150 °C also belongs to the *4 mm* point group, and its SHG patterns and theoretical simulations are again proved.

In summary, though plenty of studies have been done on using SHG to exhibit the phase transition in BTO[11,12,22,23] and on proving the coexistence of displacive and order-disorder dynamics in the phase transition of BTO,[3,18,24–26] the coexistence is demonstrated by SHG results in this work. Because of the difference in the initial polarization states of the polarized (001) and non-polarized (100) BTO crystals, the dominated kinetic mechanism of phase transformation around T_C is displacive for the polarized (001) BTO, while displacive and order-disorder for the other depending on the temperature variation. The out-of-plane PFM results present the increase in domain walls in BTO crystals after annealing, which we believe is the reason for the corresponding excess SH signal measured, as different polarizations on each side of the domain walls break the inversion symmetry, which contributes to the SHG signal reflected from the surface for polarized BTO.

This work was supported by the National Key Basic Research Program of China (Grants Nos. 2014CB921001 and 2017YFA0303604), the National Natural Science Foundation of China (Grants Nos. 11721404, 51761145104, and 11674385), the Key Research Program of Frontier Sciences of the Chinese Academy of Sciences (Grant No. QYZDJ-SSW-SLH020), and the Strategic Priority Research Program (B) of the Chinese Academy of Sciences (Grant No. XDB07030200).

[1]K. A. Müller and W. Berlinger, Phys. Rev. B **34**, 6130 (1986).
[2]A. Bussmann-Holder, H. Beige, and G. Völkel, Phys. Rev. B **79**, 184111 (2009).
[3]B. Zalar, V. V. Laguta, and R. Blinc, Phys. Rev. Lett. **90**, 037601 (2003).
[4]J. S. Wang, K. J. Jin, J. X. Gu, Q. Wan, H. B. Yao, and G. Z. Yang, Sci. Rep. **7**, 9051 (2017).
[5]O. Trithaveesak, J. Schubert, and C. Buchal, J. Appl. Phys. **98**, 114101 (2005).
[6]Y. J. Chang, New Phys.: Sae Mulli. **64**, 15 (2014).
[7]H. Akamatsu, K. Fujita, T. Kuge, A. S. Gupta, A. Togo, S. M. Lei, F. Xue, G. Stone, J. M. Rondinelli, L. Q. Chen, I. Tanaka, V. Gopalan, and K. Tanaka, Phys. Rev. Lett. **112**, 187602 (2014).
[8]S. W. Kim, Z. Deng, M. R. Li, A. S. Gupta, H. Akamatsu, V. Gopalan, and M. Greenblatt, Inorg. Chem. **55**, 1333 (2016).
[9]L. M. Garten, M. Burch, A. S. Gupta, R. Haislmaier, V. Gopalan, E. C. Dickey, and S. T. McKinstry, J. Am. Ceram. Soc. **99**, 1645 (2016).
[10]M. Fiebig, V. V. Pavlov, and R. V. Pisarev, J. Opt. Soc. Am. B **22**, 96 (2005).
[11]A. M. Pugachev, V. I. Kovalevskii, N. V. Surovtsev, S. Kojima, S. A. Prosandeev, I. P. Raevski, and S. I. Raevskaya, Phys. Rev. Lett. **108**, 247601 (2012).
[12]V. I. Kovalevskii, V. K. Malinovskii, A. M. Pugachev, I. P. Raevskii, S. I. Raevskaya, P. D. Rudych, and N. V. Surovtsev, Phys. Solid State **54**, 920 (2012).
[13]J. S. Wang, K. J. Jin, H. Z. Guo, J. X. Gu, Q. Wan, H. X. X. L. Li, X. L. Xu, and G. Z. Yang, Sci. Rep. **6**, 38268 (2016).
[14]Y. R. Shen, *The Principles of Nonlinear Optics* (Wiley, New York, 1984).
[15]T. Zhao, F. Chen, H. B. Lv, G. Z. Yang, and Z. H. Chen, Sci. China A **43**, 760 (2000).
[16]C. J. Long, D. Ebeling, S. D. Solares, and R. J. Cannara, J. Appl. Phys. **116**, 124107 (2014).
[17]W. Cochran, Adv. Phys. **9**, 387 (1960).
[18]M. S. Senn, D. A. Keen, T. C. A. Lucas, J. A. Hriljac, and A. L. Goodwin, Phys. Rev. Lett. **116**, 207602 (2016).
[19]G. R. Fox, J. K. Yamamoto, D. V. Miller, L. E. Cross, and S. K. Kurtz, Mater. Lett. **9**, 284 (1990).
[20]W. Prusseit-Elffroth and F. Schwabl, Appl. Phys. A **51**, 361 (1990).
[21]R. Q. Zhao, K. J. Jin, H. Z. Guo, H. B. Lu, and G. Z. Yang, Sci. China Phys., Mech. Astron. **56**, 2370 (2013).
[22]A. M. Pugachev, V. I. Kovalevskii, V. K. Malinovsky, and N. V. Surovtsev, "Ferroelectric phase transition in nanostructured $BaTiO_3$ studied by Raman scattering and second harmonic generation" (IEEE, 2013), Vol. 87, ISBN: 978-1-4673-5996-2.
[23]A. Q. Jiang, J. F. Scott, H. B. Lv, and Z. H. Chen, J. Appl. Phys. **93**, 1180 (2003).
[24]A. Pramanick, X. P. Wang, C. Hoffmann, S. O. Diallo, M. R. V. Jørgensen, and X. L. Wang, Phys. Rev. B **92**, 174103 (2015).
[25]E. A. Stern, Phys. Rev. Lett. **93**, 037601 (2004).
[26]Q. S. Zhang, T. Cagin, and W. A. Goddard III, PNAS **103**, 14695 (2006).